

University of Groningen

The influence of the crystal lattice on coarsening in unstable epitaxial growth

Ahr, M.; Biehl, M.; Kinne, M.; Kinzel, W.

Published in:
Surface Science

DOI:
[10.1016/S0039-6028\(00\)00725-1](https://doi.org/10.1016/S0039-6028(00)00725-1)

IMPORTANT NOTE: You are advised to consult the publisher's version (publisher's PDF) if you wish to cite from it. Please check the document version below.

Document Version
Publisher's PDF, also known as Version of record

Publication date:
2000

[Link to publication in University of Groningen/UMCG research database](#)

Citation for published version (APA):

Ahr, M., Biehl, M., Kinne, M., & Kinzel, W. (2000). The influence of the crystal lattice on coarsening in unstable epitaxial growth. *Surface Science*, 465, 339-346. [https://doi.org/10.1016/S0039-6028\(00\)00725-1](https://doi.org/10.1016/S0039-6028(00)00725-1)

Copyright

Other than for strictly personal use, it is not permitted to download or to forward/distribute the text or part of it without the consent of the author(s) and/or copyright holder(s), unless the work is under an open content license (like Creative Commons).

The publication may also be distributed here under the terms of Article 25fa of the Dutch Copyright Act, indicated by the "Taverne" license. More information can be found on the University of Groningen website: <https://www.rug.nl/library/open-access/self-archiving-pure/taverne-amendment>.

Take-down policy

If you believe that this document breaches copyright please contact us providing details, and we will remove access to the work immediately and investigate your claim.

Downloaded from the University of Groningen/UMCG research database (Pure): <http://www.rug.nl/research/portal>. For technical reasons the number of authors shown on this cover page is limited to 10 maximum.

The influence of the crystal lattice on coarsening in unstable epitaxial growth

M. Ahr^{a,*}, M. Biehl^a, M. Kinne^b, W. Kinzel^a

^a Institut für Theoretische Physik, Julius-Maximilians-Universität Würzburg, Am Hubland, D-97074 Würzburg, Germany

^b Lehrstuhl für Physikalische Chemie II, Egerlandstr. 3, D-91058 Erlangen, Germany

Received 2 June 2000; accepted for publication 13 June 2000

Abstract

We report the results of computer simulations of epitaxial growth in the presence of a large Schwoebel barrier on different crystal surfaces: simple cubic(001), bcc(001), simple hexagonal(001) and hcp(001). We find that mounds coarsen by a step-edge diffusion-driven process, if adatoms can diffuse relatively far along step edges without being hindered by kink-edge diffusion barriers. This yields the scaling exponents $\alpha = 1$, $\beta = \frac{1}{3}$. These exponents are independent of the symmetry of the crystal surface. The crystal lattice, however, has strong effects on the morphology of the mounds, which are by no means restricted to trivial symmetry effects. Whereas we observe pyramidal shapes on the simple lattices, on bcc and hcp there are two fundamentally different classes of mound, which are accompanied by characteristic diffusion currents: a metastable one with rounded corners, and an actively coarsening configuration, which breaks the symmetry given by the crystal surface. © 2000 Elsevier Science B.V. All rights reserved.

Keywords: Growth; Monte Carlo simulations; Surface structure, morphology, roughness, and topography

1. Introduction

In spite of considerable efforts [1–7], see Ref. [8] for an overview, a thorough theoretical understanding of the late phases of epitaxial crystal growth is still lacking. In this publication we investigate the problem of growth in the presence of a strong Schwoebel barrier, which hinders interlayer transport and leads to an instability of the flat surface. During an initial transient, *mounds* form on the surface, which then start to merge. It is generally accepted that in this asymptotic *coarsening* regime the statistical properties of the surface remain invariant under a simultaneous transforma-

tion of spatial extension x , height $h(x)$ and time t :

$$x \rightarrow bx; h(x) \rightarrow b^z h; t \rightarrow b^x t, \quad (1)$$

where α and $\beta := \alpha/z$ are believed to be *universal* exponents, which do not depend on details of the model, and b is an arbitrary factor. If the process of growth stabilizes a specific slope, this will yield $\alpha = 1$.

It was first pointed out by Siegert and coworkers [3,4] that lattice symmetries may play an important role in the coarsening process. These authors investigated continuum equations, using an analogy between coarsening and a phase ordering process, which has recently gained popularity [9]: areas of constant slope should correspond to domains of a constant order parameter. They derived scaling exponents $\alpha = 1$, $\beta = \frac{1}{3}$ on surfaces with a triangular

* Corresponding author. Fax: +49 931 8885141.
E-mail address: ahr@physik.uni-wuerzburg.de (M. Ahr)

symmetry, and $\beta = 1/(3\sqrt{2}) \approx 0.24$ for generic cubic surfaces, while $\beta = \frac{1}{3}$ requires a fine-tuning of parameters. However, Monte Carlo simulations have raised doubts on these predictions, since they yield $\beta \approx \frac{1}{3}$ on cubic surfaces for a great range of parameters, e.g. see Refs. [10–13]. In this paper, we want to address the following questions. (1) What are the *mesoscopic* processes that make the mounds coarse? (2) How does the coarsening process depend on the crystal lattice and its symmetries? (3) Do these results support a deeper analogy between coarsening and phase ordering?

2. The model

To answer these questions, we perform computer simulations of growth on (001) surfaces of the simple cubic (sc) lattice, the simple hexagonal (sh) lattice, the body-centred cubic (bcc) lattice and for hexagonal close packing (hcp). This is done under solid-on-solid conditions, i.e. the effects of overhangs or dislocations are being neglected. Then, the simple lattices can be represented by a square (sc) or a triangular mesh (sh) of integers, which denote the height $h(\mathbf{x})$ of the surface. We build the bcc (hcp) lattice out of two intersecting sc (sh) sublattices, one of which contains the even heights and the other the odd heights.¹ Here, an adatom in a *stable* configuration is bound to four (three) neighbours below in the other sublattice, which will be denoted as *vertical neighbours* in the following. Particles with fewer vertical neighbours form overhangs, which are forbidden by the solid-on-solid condition. This is physically reasonable, since such particles are only weakly bound and, therefore, these configurations will be unstable. Additionally, particles may have neighbours in the *lateral* direction that are in the same sublattice.

The investigation of the coarsening process requires a fast algorithm that allows for the simulation of the deposition of thick films on comparatively large systems. Standard kinetic Monte Carlo

techniques, which consider the moves of many particles on the surface simultaneously (full diffusion models), require computationally expensive bookkeeping procedures. This makes them too slow for our purpose. Instead, we simulate the moves of a *single* particle from deposition until an immobile state is reached [10,11]: an adatom impinges on a randomly chosen lattice site. Owing to its momentum perpendicular to the surface, the particle may funnel downhill [14–16] to the lowest (vertical) neighbour site. On bcc and hcp this is repeated until it reaches a *stable site*, as defined above. On the simple lattices this is a site \mathbf{x} , where all nearest neighbour sites have a height $\geq h(\mathbf{x})$. Then, the adatom diffuses on the surface. If the particle has no lateral neighbours, one of its neighbour sites is chosen at random. On the simple lattices, the particle moves to this site only if its height does not change, i.e. we introduce an infinite Schwoebel barrier. On the bcc or hcp lattice, the particle is moved to the neighbour site if it is stable. This condition also implies an infinite Schwoebel barrier, since a transition into a different layer can proceed only via a weakly bound (unstable) transient state. This procedure is repeated until either a lateral neighbour is reached or l_d^2 steps have been performed. The simulation of single particles requires an effective representation of the collisions of diffusing adatoms that form a stable nucleus. The diffusion length l_d corresponds to the mean free path and depends on the diffusion constant D and the particle flux F : $l_d \propto (D/F)^{1/6}$ [17]. Note that in our model l_d fixes only the number of mounds that form initially, i.e. it represents the typical distance of nucleation events. In the later stages of growth the typical terrace width is much smaller than l_d and nucleation is negligible.

As soon as a particle has a lateral neighbour, it is bound to it. This process is irreversible, in the sense that we forbid diffusion processes that reduce the number of bonds, like the detachment from a step edge. However, the adatom may diffuse along the edge. After l_k^2 steps, or if the particle has reached a kink site, it is fixed to the surface. If not stated otherwise, diffusion around corners is allowed. Analogous to planar diffusion, l_k represents the typical distance of nucleation in the

¹ For simplicity, we assume the spacing between the layers to be one lattice constant. Our algorithm depends only on the *topology* of the lattice.

effectively one-dimensional step edge diffusion, see Ref. [17] for a discussion.

Within this model, we measure time t in units of the time needed to deposit a monolayer. This algorithm may be programmed very efficiently and is about an order of magnitude faster than full diffusion Monte Carlo algorithms. The two essential simplifications in our model are (a) the effective representation of nucleation events in a single particle dynamics and (b) the consideration of irreversible processes, i.e. infinite energy barriers for detachment and downward diffusion at edges. For the simple cubic lattice, the model was studied in Refs. [10–12] with particular emphasis on the role of step edge diffusion. In Ref. [12] a full diffusion model is considered for comparison, which includes detachment as well as finite Schwoebel barriers and displays the same asymptotic coarsening exponents as measured in the simplified model.

In all our simulations we choose $l_d = 15$, which sets the initial island distance. We simulate a variety of different values of the step edge diffusion length l_k in the range between $l_k = 1$ and $l_k = 20$. The simulations are performed on a square of $N \times N$ lattice constants using periodic boundary conditions (bcc and sc), and a regular hexagon with edges of length M (hcp and sh) using helical boundary conditions, our standard values being $N = 512$ and $M = 300$. For every parameter set, we have performed seven independent simulation runs.

3. Surface morphologies

During the first (about 100) monolayers of growth on an initially flat surface, islands nucleate, on which mounds build up and take on their stable slope. Then, the asymptotic coarsening regime starts. As expected, on the simple lattices the mounds obtain regular shapes, which are determined by the symmetry of the surface: square pyramids on sc, hexagonal ones on sh. On bcc and hcp, however, *rounded* corners as well as sharp corners can be found (Figs. 1b and 2). Here one finds two fundamentally different types of mound. On the one hand, there are mounds where *all*

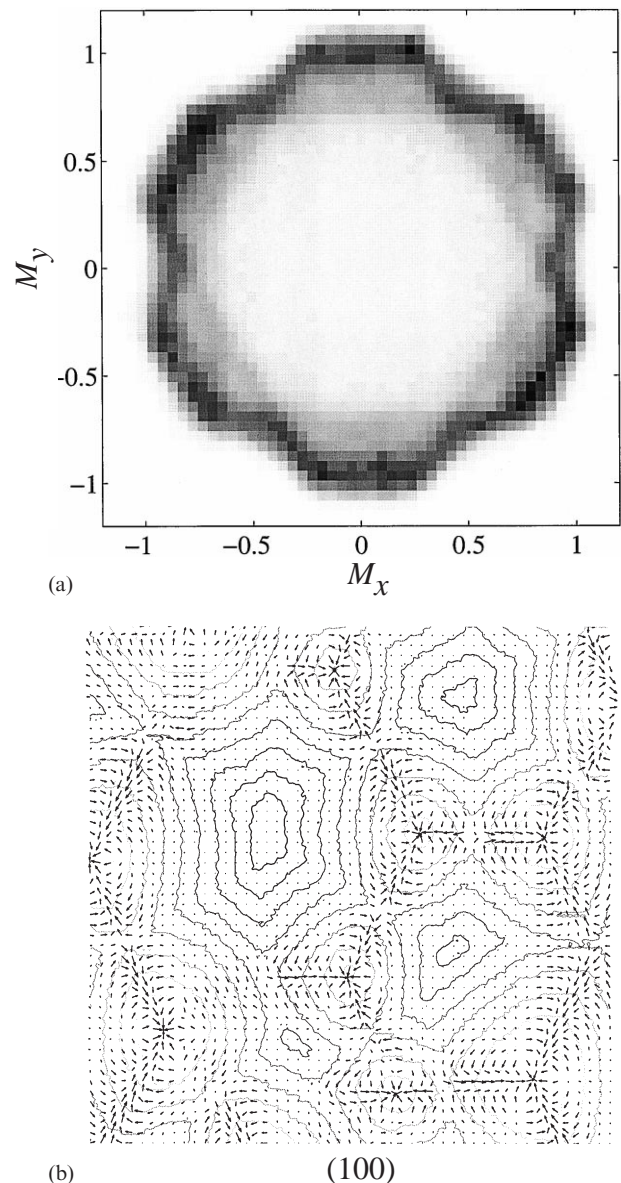


Fig. 1. Simulation results on hcp ($M = 300$, $l_d = 15$, $l_k = 10$, $t = 20\,000$ ML). (a) Histogram of slopes (density plot). High probabilities are drawn dark. (b) Contour plot of a part of size 250×250 lattice constants of the surface. High levels are plotted in light grey. The arrows show the surface current, as measured during deposition of an additional 200 ML.

corners are rounded with octagonal shapes on bcc (Fig. 2b), and 12-cornered ones on hcp. On the other hand, one observes a *breaking* of the symmetry given by the lattice: approximately triangular

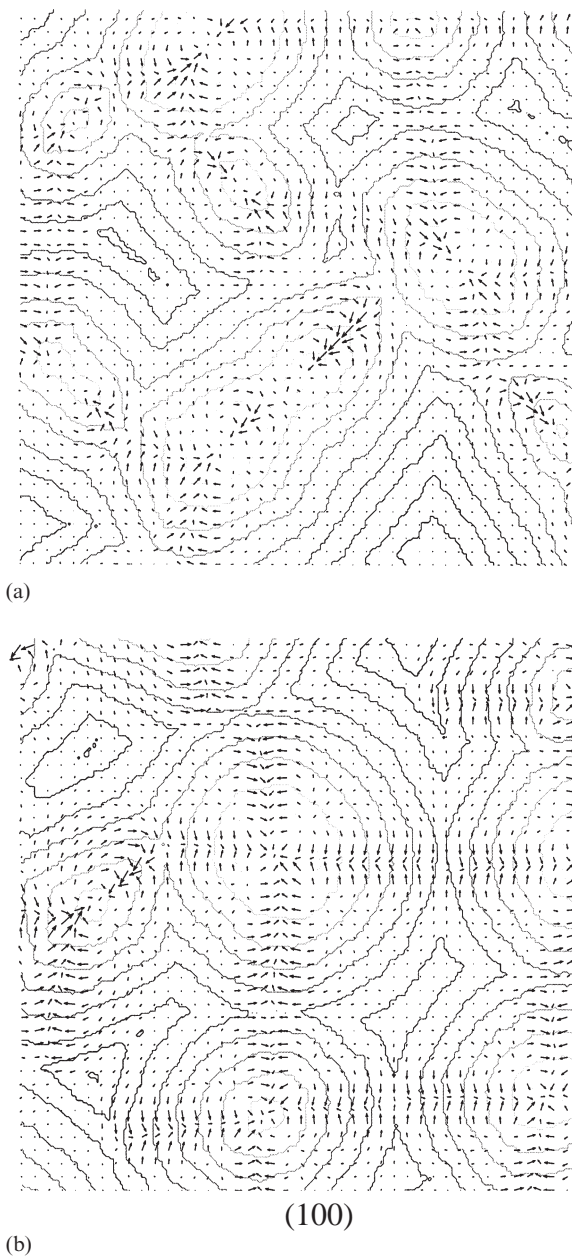


Fig. 2. Contour plots of parts of size 250×250 lattice constants of bcc surfaces ($N=512$, $l_d=15$, $l_k=10$, $t=20\,000$ ML). (a) Section dominated by quickly coarsening mounds breaking the surface symmetry. (b) Metastable configuration.

mounds on hcp (Fig. 1b) and oval shapes on bcc (Fig. 2a), where every second one of the corners is sharp, while the others are rounded. In the

process of coarsening, we have observed that on all lattice structures the mounds merge preferentially at the *corners*, while mounds touching at the flanks are a *metastable* configuration. On bcc and hcp the metastable configuration is made of mounds with completely rounded corners. Mounds whose shapes break the lattice symmetry are always in the course of merging with a neighbour they touch with a sharp corner.² Note that similar configurations were observed in a full diffusion simulation of bcc(001) growth [13].

To characterize the morphology quantitatively, we investigate the slopes $\mathbf{m} = \nabla h$ of the surface. On average, $|\mathbf{m}|$ obtains a value that can be estimated by a simple argument [18]: the Schwoebel effect yields an uphill current due to the preferential attachment of particles on terraces from below, which is compensated by a downhill current due to funnelling. If we assume that a particle reaches its final height after, at most, one incorporation step, the sc and the sh surfaces select $|\mathbf{m}| = \frac{1}{2}$, whereas bcc and hcp select $|\mathbf{m}| = 1$. In practice, the selected slopes are slightly smaller, since the maximal number of incorporation steps in the funneling process is unlimited. Since a direct computation of the numerical gradient of simulated surfaces fails due to the discrete heights, we first apply a Gaussian filter with variance $\sigma=4$. This value has turned out to be a good compromise: it removes the atomistic structure, but preserves the shape of the mounds. Fig. 1a shows a two-dimensional histogram of the slopes on hcp surfaces; owing to the round shapes of the mounds, one finds a pronounced maximum of the probability density function in every direction of \mathbf{m} . The most probable value of $|\mathbf{m}|$ has a directional dependence: it is *minimal* in the lattice directions (0.88 ± 0.02), and *maximal* (0.99 ± 0.02) in the intermediary directions. Consequently, the rounded corners are *steeper* than the flanks. This is possible because the rounding occurs at the base of the mounds, whereas close to the tips the corners are typically sharp, see Fig. 2. On bcc the results are equivalent, apart from the different symmetry,

² MPEG videos of our simulations are available on-line at <http://theorie.physik.uni-wuerzburg.de/~ahr/LATTICE/lattice.html>.

whereas they are rather trivial on sc and sh: a regular square and hexagon respectively of slightly broadened peaks, which correspond to the flanks of the mounds.

4. Diffusion currents

In order to gain deeper insight into the coarsening process, we investigate the *material transport* on mesoscopic length scales by tracing the motion of particles on the surface. On all lattice structures we observe a strong uphill current at the corners of mounds, which is a geometrical effect: an adatom attaching at the corner is transported over a mean distance l_k , namely with equal probability along either of the two flanks of the mound. This results in a net current j in the direction of the bisector of the angle at the corner, which is directed uphill. A simple calculation yields

$$|j| = r_a l_k \cos \frac{\phi}{2}$$

if there is a straight step edge of length very much greater than l_k , which is the case on the simple lattices. Here r_a is the rate with which particles attach at a step edge, $\phi = \pi/2$ on surfaces with cubic symmetry and $\phi = 2\pi/3$ on hexagonal surfaces. On the bcc and the hcp lattice, however, material transport along step edges is severely restricted due to the rounded corners. There, particles diffusing along the step edge are typically *reflected*, which leads to a current towards the middle of the smooth step edges at the flanks of mounds in the metastable configuration, which have an extension $\sim l_k$ (Fig. 2b). This current has a non-vanishing *uphill* component due to the Schwoebel effect. On the rounded corners on the contrary, one observes a weak *downhill* current. This is explained by the observation of steep gradients (Fig. 1a), at which the downhill current due to funnelling dominates the uphill current of the Schwoebel effect. On these surfaces the stable slope, at which the currents cancel, is *not* assumed *locally*, but only in the *global* average, which results in spatial current patterns on the surface. An analogous behaviour is observed at the symmetry-

breaking merging mounds (Figs. 1b and 2a). Here, the smooth edges are in the proximity of the sharp corners. Particles are reflected at the rounded corners, too. This yields a net current towards the sharp corners, which *compensates* the geometrically induced uphill current exactly, if the smooth edges have a length l_k . This fact explains the broken symmetry of these mounds: if there is any process that transports matter towards sharp corners, then this material is not completely diffusing inward, as would be the case on pyramidal mounds, but is attached to the corner and makes it overgrow its neighbours. Merging of mounds, however, *is* such a process. Consider a terrace, which goes around two mounds touching each other at the corners. Owing to its curvature, in this contact zone there is a high concentration of kink sites, which make it a *sink* for diffusing particles.

5. Theoretical estimation of scaling exponents

Our observation that mounds merge preferentially in positions with touching corners provides strong evidence that the current that fills the gap between two mounds plays a dominant role in the process of coarsening, at least in the case of large l_k , where it is efficient. If this is the case, then a simple consideration yields the scaling exponents: owing to step edge diffusion, adatoms are transported over a typical distance l_k . If l_k is noticeably greater than a few lattice constants, this is much larger than the average terrace width. Then, material transport via diffusion on terraces is small compared with transport via step edge diffusion and can be neglected. Fig. 1b shows that the current into the gap is significant on a few atomic layers in the vicinity of the contact point only. In consequence, this current is *independent* of the size of the mounds, if the latter is much greater than l_k . Since the volume of the gap is proportional to L^3 , if L is the typical distance between the mounds, it will take a time $t \approx L^3$ to fill it. In consequence, $L \approx t^{1/3} \Rightarrow z = 3$. Since $\alpha = 1$ in the presence of slope selection, this yields $\beta = \frac{1}{3}$. In contrast to the effects discussed in Refs. [3,4], these considerations are completely independent of lattice symmetries. In

Refs. [5,6] a similar argument has been applied to the case of coarsening in the absence of dominant step edge diffusion processes ('bond-energy-driven coarsening'), where material is transported mainly by terrace diffusion. This yields $\beta = \frac{1}{4}$. The same exponent is obtained, if coarsening is exclusively due to fluctuations in the particle beam ('noise-assisted coarsening'). We expect that these processes dominate step edge diffusion in the limit of small l_k , which leads to a transient from $\beta = \frac{1}{4}$ to $\beta = \frac{1}{3}$ when l_k is increased.

6. Measurement of scaling exponents

We apply a variety of methods to measure the scaling exponents. This is important as a consistency check and to eliminate systematic errors that might be intrinsic to some methods. First, β can be obtained from the increase of the *surface width* $w(t) = \langle [h(\mathbf{x}, t) - \langle h \rangle(t)]^2 \rangle^{1/2}$ with time. Eq. (1) corresponds to $w(t) \approx t^\beta$ [19]. This power law behaviour may be corrupted by the presence of noise on the surface profile, an additional contribution to $w(t)$ which has been called *intrinsic width* [19,20]. Similarly, the number of mounds n_m in the system will decrease like $t^{-2/z}$, if this scaling hypothesis holds. We measure n_m by counting the number of top terraces in the system. Since a single particle is counted as a terrace, this method may be misleading if particles nucleate on terraces at the flanks of mounds. A method that is widely used in the literature uses the Fourier transform $\hat{h}(\mathbf{k})$.³ The structure factor $S(\mathbf{k}) := \langle \hat{h}(\mathbf{k}) \hat{h}(-\mathbf{k}) \rangle$ will be maximum at non-zero wave numbers $|\mathbf{k}_m| = 2\pi/l_m$, if there are structures at a typical length scale l_m on the surface. Since $l_m \approx t^{1/z}$, $|\mathbf{k}_m|$ will decay $\sim t^{-1/z}$. In practice, a direct search for the maximum often fails owing to noise effects; one avoids this problem by calculating the averages

$$k_m^{(p)} := \langle [\sum_{\mathbf{k}} |\mathbf{k}| S(\mathbf{k})^p] / \sum_{\mathbf{k}} S(\mathbf{k})^p \rangle;$$

however, the choice of the correct power p is a bit arbitrary.

³ The mean surface height is subtracted before performing the Fourier transform.

6.1. The wavelet method

To avoid these difficulties, we propose a method that exploits the continuous wavelet transform

$$T_{\Psi}[h](\mathbf{b}, a) := \frac{1}{a} \int d^2x \left\{ \frac{\Psi_1[(\mathbf{x} - \mathbf{b})/a]}{\Psi_2[(\mathbf{x} - \mathbf{b})/a]} \right\} h(\mathbf{x}) \quad (2)$$

of the surface heights. Here, the wavelets Ψ_1 and Ψ_2 are defined as partial derivatives of a radially symmetric filter $\phi(\mathbf{x})$, which we choose to be a Gaussian: $\Psi_1 := \partial\phi/\partial x$, $\Psi_2 := \partial\phi/\partial y$. The basic idea of this transform is to convolve $h(\mathbf{x})$ with the wavelets, which are *dilated* with the scale a . This makes it a natural tool to search for the typical length scale a_t of structures on the surface. In Refs. [21,22], it has been proposed to investigate the *wavelet transform modulus maxima* (WTMM). They are defined as local maxima of the *modulus* $M_{\Psi}[h](\mathbf{b}, a) := |T_{\Psi}[h](\mathbf{b}, a)|$ in the direction of T_{Ψ} . The search for the WTMM is equivalent to *edge detection*: they lie on connected curves, which trace the contours of objects of size $\sim a$. We investigate the average of the WTMM on the scale a

$$W_m(a) := \langle M_{\Psi}[h](\mathbf{b}, a) \rangle_{\mathbf{b} = \text{WTMM}}.$$

This function has a pronounced maximum at a value $a_m \propto a_t$, which is the scale that contains the most relevant contributions to the surface morphology. On mounded surfaces, $a_m \approx t^{1/z}$ is proportional to the *lateral size* of the mounds, while $W_m(a_m) \approx t^\beta$ is a measure for their heights. This procedure has several advantages compared with the standard methods used in the literature. (1) The detection of the WTMM leads to an efficient suppression of noise, and therefore eliminates the (noisy) intrinsic width. (2) Since only the most important length scale is considered, the results may not be corrupted by details of the surface morphology on small length scales. (3) Appropriate wavelets are well localized both in real space and in Fourier space. Therefore, this analysis combines the advantages of both real-space techniques, like the counting on mounds, and Fourier techniques, like the calculation of k_m^p . We have tested it both with artificial test surfaces and various toy models of growth and found a clear superiority to the standard methods,

especially in the presence of noise, which should make it interesting for experimental investigations. Details will be given in a forthcoming publication.

6.2. Results

In our simulations, the asymptotic scaling behaviour is obtained after a long initial transient of about 100 monolayers. Since after this transient only a comparatively small number of mounds is left on the surface, the measurement of exponents is complicated by finite size effects: owing to the periodicity of the system, there is a *self-interaction* of the currents on the mounds, if their size is no longer small compared with the system size. We measure $\alpha \approx 1$ for all $l_k > 1$, a consequence of slope selection. At $l_k = 1$, however, we measure smaller values, which *do* depend on the crystal lattice: $\alpha = 0.85$ on bcc and $\alpha = 0.94$ on hcp. A similar effect was observed in Refs. [10,11] on the simple cubic lattice. We remark that our results are independent of the method applied to measure the exponents. In Fig. 3, β is plotted as a function of l_k . Clearly, its value does *not* depend systematically on the *symmetry* of the crystal surface. We find no significant deviations between β on bcc and on hcp (sc

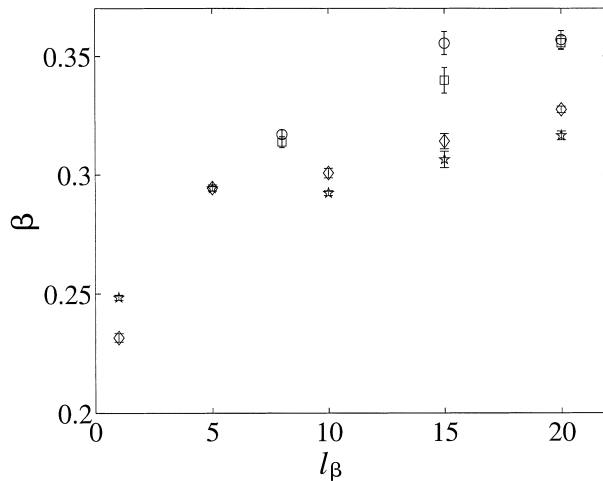


Fig. 3. β , as obtained from the wavelet method, as a function of the step edge diffusion length. Diamonds: bcc lattice, squares: sc, stars: hcp, circles: sh. Results from measurements of β from the surface width are identical within the error bars. These have been estimated from the logarithmic fits; we expect the true errors to be larger due to systematic deviations.

and sh). As already observed in Refs. [10,11], there is a dependence of β on the step edge diffusion length. One obtains values $\sim \frac{1}{4}$ at $l_k = 1$ and higher values at greater l_k . The values obtained at large l_k are compatible with $\beta = \frac{1}{3}$. As indicated above, we explain this transient as a competition between different coarsening mechanisms. At large l_k the merging of mounds should proceed mainly by the step-edge diffusion-driven transport of material into the gap; at small l_k it is dominated by noise-assisted coarsening and/or bond-energy-driven coarsening. This competition might also explain why the exponents measured on bcc and hcp are still slightly smaller than those obtained on the simple lattices, even at values of l_k as large as 20, since the symmetry breaking of the mounds on these lattices halves the number of corners that are active in the coarsening process. All the simulation results reported above have been obtained in simulations with unhindered step edge diffusion. To corroborate further our ideas of the coarsening process, we have also performed simulations with a corner diffusion barrier. A particle may diffuse at most l_k steps along a straight step edge, but diffusion around corners is forbidden. Then, we observe *no symmetry breaking* of the mounds, which now obtain regular polygonal shapes on all lattice structures. These are rotated by an angle of 45° against the lattice directions on cubic surfaces and 30° on hexagonal ones. Owing to the absence of aligned step edges, material transport by step edge diffusion is severely restricted under these conditions. Thus, we measure only small diffusion currents, and observe no pronounced long-range order in the flux lines. Here, we find $\alpha \approx 1$, $\beta \approx \frac{1}{4}$ on *all* lattices, *independent* of the step edge diffusion length. This slow coarsening in the absence of the characteristic features of step-edge diffusion-driven coarsening — currents on mesoscopic length scales and symmetry breaking on bcc and hcp — strongly supports the important role of this mechanism for fast coarsening with $\beta = \frac{1}{3}$.

7. Conclusions

In summary, we have presented a detailed investigation of the coarsening process in epitaxial

growth. Our most important finding is that the crystal lattice has a considerable influence on the morphology of the growing surface, which is by no means restricted to trivial symmetry effects. In spite of these differences, in the limit of large step edge diffusion lengths, the mounds coarsen according to power laws with universal exponents. We obtain $\beta \approx \frac{1}{3}$ in the case of unhindered step edge diffusion. In the case of restricted step edge diffusion, $\beta \approx \frac{1}{4}$ is observed as it is for unhindered step edge diffusion with a small value of l_k . This effect of an additional barrier at corners was previously observed in Refs. [10,11] for the simple cubic lattice and in Ref. [13] for the bcc(001) system.

Clearly, the single particle dynamics cannot reproduce full diffusion simulations in every detail. However, the potential influence of the lattice symmetry on the coarsening dynamics and its characteristic exponents should not be affected crucially by the simplifications of our model.

Our results contradict previous studies of the coarsening process using continuum equations [2–4], which predict slower coarsening on surfaces with a cubic symmetry. In these publications, equations have been studied that are invariant under the transformation $h(\mathbf{x}) \rightarrow -h(\mathbf{x})$. This symmetry reflects itself also in the up–down symmetry of the solutions of the equations. Clearly, our simulation results *break* this symmetry and the arguments of [2–4] cannot apply here. In Figs. 1a and 2 the contours of the mounds and those of the valleys are clearly distinct. This is also true for the *currents*, especially the step edge diffusion current, which dominates the coarsening behaviour in the limit of large l_k and unhindered step edge diffusion and determines the scaling exponents. We conclude, that the breaking of the up–down symmetry is a central feature of unstable epitaxial growth. Its precise effect on the coarsening dynamics clearly deserves further attention. However, we find it difficult to interpret our result in the context of an analogy to phase ordering processes, where the local slope of the surface corresponds to an order parameter. In this picture, the importance of the breaking of up–down symmetry leads to the conclusion that, now, the stability of a domain wall between areas of equal slope is a complicated function of both the *orienta-*

tion of the wall and the *order parameters* on both sides of it. Additionally, in contrast to the simple lattices, where there are only four (sc) or six (sh) stable slopes, on bcc and hcp one would have to deal with a *continuous* order parameter.

In any case, the behaviour of our models, which implement the microscopic processes on the surface, is governed by much more complex rules than those implemented in all the continuum models we are aware of. Differences are by no means restricted to some details, but have a fundamental influence on the behaviour of the system on large length scales.

References

- [1] M. Kalf, P. Smilauer, G. Comsa, T. Michely, Surf. Sci. 426 (1999) L447.
- [2] M. Rost, J. Krug, Phys. Rev. E 55 (1997) 3952.
- [3] M. Siegert, M. Plischke, R.K.P. Zia, Phys. Rev. Lett. 78 (1997) 3705.
- [4] M. Siegert, Phys. Rev. Lett. 81 (1998) 5481.
- [5] L.-H. Tang, P. Smilauer, D.D. Vvedensky, Eur. J. Phys. B 2 (1998) 409.
- [6] L.-H. Tang, Physica A 254 (1998) 135.
- [7] D.E. Wolf, in: A.J. McKane (Ed.), Scale Invariance Interfaces and Non-Equilibrium Dynamics, Plenum, 1995., Proceedings of NATO Advanced Study Institute, Cambridge, June 1994.
- [8] P. Politi, G. Grenet, A. Marty, A. Pouchet, J. Villain, Phys. Rep. 324 (5–6) (2000) 271.
- [9] J. Krug, M. Schimschak, J. Phys. I (Fr.) 5 (1995) 1065.
- [10] M. Biehl, M. Kinne, W. Kinzel, S. Schinzer, Proceedings of the 1998 Conference on Computational Physics, Comput. Phys. Commun. 121–122 (1999) 347.
- [11] S. Schinzer, M. Kinne, M. Biehl, W. Kinzel, Surf. Sci. 439 (1999) 191.
- [12] S. Schinzer, M. Sokolowski, M. Biehl, W. Kinzel, Phys. Rev. B 60 (1999) 2893.
- [13] J.G. Amar, Phys. Rev. B 60 (1999) R11317.
- [14] J.W. Evans, D.E. Sanders, P.A. Thiel, A.E. DePristo, Phys. Rev. B 41 (1990) 5410.
- [15] J.W. Evans, Phys. Rev. B 43 (1991) 3897.
- [16] Y. Yue, Y.K. Ho, Z.Y. Dan, Phys. Rev. B 57 (1998) 6685.
- [17] J. Villain, A. Pimpinelli, L. Tang, D. Wolf, J. Phys. I (Fr.) 2 (1992) 2107.
- [18] J. Krug, M. Siegert, M. Plischke, Phys. Rev. Lett. 70 (1993) 3271.
- [19] A.-L. Barabási, H.E. Stanley, Fractal Concepts in Surface Growth, Cambridge University Press, Cambridge, 1995.
- [20] J. Kertész, D.E. Wolf, J. Phys. A: Math. Gen. 21 (1988) 747.
- [21] S. Mallat, W.L. Hwang, IEEE Trans. Inf. Theory 38 (1992) 617.
- [22] S. Mallat, S. Zhong, IEEE Trans. Pattern Anal. Mach. Intell. 14 (1992) 710.